

Probabilistic analysis of a partially-restrained steel-concrete composite frame

C. Amadio*

*Department of Civil and Environmental Engineering, University of Trieste,
Piazzale Europa 1, 34127 Trieste, Italy*

Abstract. The paper investigates the seismic performance of a Partially-Restrained (PR) steel-concrete composite frame using the probabilistic approach. The analysed frame was tested at the ELSA laboratory of the Joint Research Centre of Ispra (Italy), while the representative beam-to-column composite connections were tested at the Universities of Pisa, Milan and Trento (Italy). The component modelling of both interior and exterior composite joints is described first, including the experimental-numerical validation. The Latin Hypercube method has been used to draw the probabilistic distribution curves of joints, and then the whole PR composite frame has been analysed. Pushover and incremental dynamic analyses have been carried out using the non-linear FE code SAP2000 version 9.1. The fragility and performance curves of the PR composite frame have been determined for four damage limit states.

Keywords: fragility curves; Latin Hypercube method; probabilistic approach; composite structures.

1. Introduction

Modern codes for design in earthquake-prone regions (FEMA 356 2000, Bertero 2002, Eurocode 8 2004) require the structure to satisfy some performance objectives during the service life. This design philosophy, known as Performance Based Seismic Design (*PBSD*), combines some structural performance levels with pre-fixed intensities of the seismic action.

The SEAOC (1995), FEMA 273 (1997) and FEMA 356 (2000), suggest four performance levels: “Fully Operational, LS0”, “Operational, LS1”, “Life Safe LS2”, and “Near Collapse, LS3”. Any performance level corresponds to a limitation of a parameter representative of a given damage limit state for structural and non-structural elements. Four design values of the seismic action, corresponding to different return periods T , also are in general defined; for example by the SEAOC these are: frequent ($T = 43$ years), occasional ($T = 72$ years), rare ($T = 475$ years), and very rare ($T = 970$ years). The design performance objectives can then be obtained by combining the aforementioned performance levels with the corresponding design values of the seismic action (Fig. 1), according to the importance of the structure (ordinary, civil defence, or special structure). The *PBSD*, therefore, requires a multi-level control by assessing the structural performance for different levels of the seismic action. The plastic behaviour is explicitly taken into account in this approach, with the aim of optimising the efficiency and the usability of the structure during the service life.

It has been recently pointed out that the use of the probabilistic approach should be preferred when evaluating the structural performance in earthquake-prone regions. The traditional deterministic

*Associate Professor, E-mail address: amadio@units.it

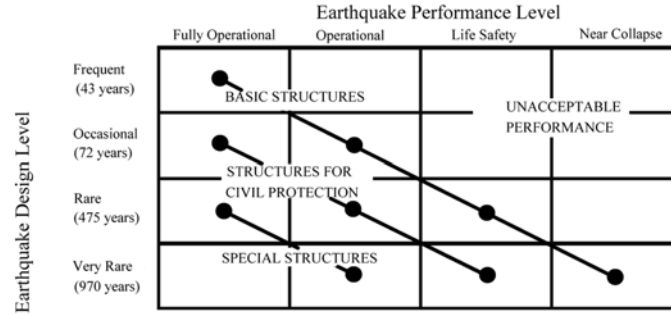


Fig. 1 Example of performance design objectives (SEAOC, Vision 2000, 1995)

approach, in fact, may lead to inconsistencies between predicted and noticed structural damages because of the uncertainties in the models used to evaluate both the demand and capacity. Conversely, the probabilistic approach can fully consider all of the uncertainties affecting the prediction of the seismic behaviour and, therefore, the actual seismic performance (Bazzurro and Cornell 1994, Dymitiotis *et al.* 1999, Cornell and Krawinkler 2000, Piluso *et al.* 2003, Altug and Elnashai 2004).

The seismic reliability of a given structural typology can be evaluated by means of the fragility curves. Such curves provide the probability of occurrence $F_r(x)$ of a given Limit State (LS), conditioned to a parameter IM representing the seismic hazard (which is usually the Peak Ground Acceleration PGA , the spectral acceleration S_a , or the spectral displacement S_d):

$$F_r(x) = P[LS|IM=x] \quad (1)$$

where the limit state LS is considered to be reached when a control variable assumes a pre-defined value. For a frame, usually the Inter-Storey Drift Angle ($ISDA$) or a damage parameter, such as the Park and Ang index (DPA), see Park and Ang (1985), are assumed as control variables. Once the fragility curves are known, the probability of failure P_f or limit state probability, can be evaluated with the formula (Cornell and Krawinkler 2000, Altug and Elnashai 2004):

$$P_f = \sum_x P[LS|IM=x] \cdot P[IM=x] = \int_0^{+\infty} H(x) \cdot \frac{dF_r(x)}{dx} dx \quad (2)$$

where $H(x)$ represents the Seismic Hazard function, generally expressed in terms of $IM=S_a$ (Song and Ellingwood 1999), according to the equation:

$$H(x) = P[S_a > x] = 1 - \exp[-(x/\mu)^{-k}] \quad (3)$$

μ and k being parameters determined according to the characteristics of the site.

Steel (Song and Ellingwood 1999, Sakurai *et al.* 2001) and concrete frames (Altug and Elnashai 2004), have been extensively analysed using the probabilistic approach.

In this paper, the seismic performance of a partially-restrained steel-concrete composite frame is investigated by following this approach. The frame, representative of a composite building in seismic zone, is realised by partially encased composite columns connected to composite beams (Bursi *et al.* 2004). The beam-to-column connections are semi-rigid with partial strength. Hereinafter the component modelling of both interior and exterior composite joints is described first, including the experimental-

numerical validation. Then the joints are fully characterized using the probabilistic approach by varying the responses of each mechanical component. The Latin Hypercube method (Olsson *et al.* 2003, Rubinstein 1981), involving less numerical analyses, is employed to draw the probabilistic distribution curves including mean values, variances and coefficients of variation.

After the joint characterisation, the whole *PR* composite frame is investigated through numerical analyses carried out by using the non-linear FE code SAP2000 version 9.1 (Computer and Structures, Inc, 2004).

The numerical model is checked against the experimental tests performed at ISPRA and then it is used to evaluate the fragility curves by means of the Latin Hypercube method. As recommended by the SAEOC, four limit states of damage are considered: “Reduced” LS0, “Limited” LS1, “Significant” LS2, and “Near Collapse” LS3. Ten earthquake ground motions, recorded at different locations, have been employed as seismic inputs. They were scaled so as to exhibit the same spectral displacement S_d for the natural vibration period of the frame. Based on results of 1500 time-history analyses, the fragility curves of the *PR* composite frame are drawn for each limit state considering the *ISDA* as damage parameter. Finally, the curves of the annual probability of failure P_f are determined for the frame in an earthquake-prone area, which is characterised by a given seismic hazard.

2. The analysed frame

The analysed frame structure, tested at the Joint Research Centre of Ispra (Bursi *et al.* 2004), represents a full-scale two-storey steel-concrete composite building. The building is made of three parallel two-bay main frames with different span lengths of 5 m and 7 m spaced 3 m one to another, with interstorey height of 3.5 m. The frames are connected in the perpendicular direction by secondary beams pinned at the ends and braced with only-tension members (Fig. 2a). The structure was designed according to the Eurocode 4 (1992) and Eurocode 8 (1996) for a *PGA* of 0.4 *g*. The composite columns, partially encased, are made of steel profiles HEB 260/280 for the exterior/interior columns, respectively. The main beams are made of an IPE 300 steel profile, connected by means of Nelson shear studs to the upper 15 cm thick concrete slab poured on a Brollo EGB 210 corrugated steel sheathing (a detailed description of the frame is reported in Bursi *et al.* 2004). The analyses have been carried out for the intermediate longitudinal frame (Fig. 2b). The frame is characterized by a fundamental period of 0.506s with a modal participant factor of 1.207, the second and third period are 0.125s, 0.035s with participant factors 0.498, 0.005, respectively.

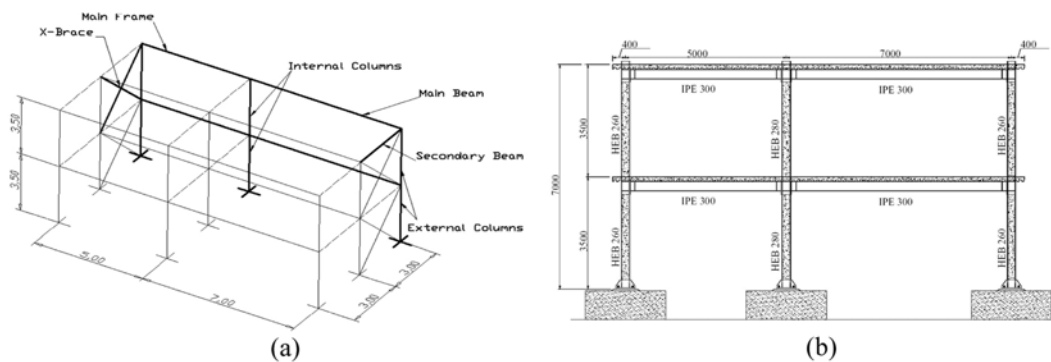


Fig. 2 The analysed structure, (a) spatial view, (b) intermediate longitudinal frame

3. The probabilistic analysis

The adopted probabilistic approach is based on the following steps:

1. definition of the most critical source of uncertainty: the seismic event;
2. modelling of the structure and beam-to-column connection, including the definition of the sources of uncertainty;
3. choice of the model used for the damage evaluation, and definition of the performance levels for the structure;
4. execution of the incremental dynamic analyses with statistical interpretation of the outcomes, and determination of the fragility, and collapse curves.

3.1 The seismic inputs

In the analysis, only recorded earthquake ground motions were used. An important point to fix in the probabilistic analysis is the number of ground motions to be considered, in order to obtain a statistically correct evaluation. Bazzurro and Cornell (1994) suggested a number of at least 5 ground motions to correctly represent the seismic hazard. Dymitiotis *et al.* (1999) recommended the use of 3 recorded ground motions at least. Recently, the use of 7 recorded ground motions have been suggested (Altug and Elnashai 2004). Since this study is aimed at the determination of the fragility curves for a structure in a generic earthquake-prone area, a number of 10 recorded earthquake ground motions has been considered. This is an optimal value as it represents a compromise between the accuracy of the analysis and the corresponding computational burden. Such ground motions have been selected so as to represent a wide range of possible seismic events of relevant intensity (magnitude ≥ 5.8). The acceleration spectra peak values correspond to different periods and they cover most periods of technical interest. The indicators of seismic intensity considered when selecting the ground motions have been:

- √ magnitude, M_s ;
- √ modified Mercalli scale MM
- √ peak ground acceleration, PGA ;

Table 1 summarizes the characteristics of the earthquake ground motions selected for the analyses. The spectral displacement S_d and spectral acceleration S_a of the selected earthquakes, computed for the structural fundamental period ($T = 0.506s$) and for a damping ratio $\xi = 5\%$, are also reported.

Table 1 Characterization of earthquake ground motions

	Earthquake	Date	Country	Station	Comp.	M_s	MM	PGA [g]	$S_d(T_1)$ [cm]	$S_a(T_1)$ [g]
GM1	Imperial Valley	15/05/1940	USA	El Centro	S00E	7.1	X/XI	0.348	5,25	0.83
GM2	Friuli	15/09/1976	Italy	Buia	N-S	6.1	IX	0.109	1.3	0.20
GM3	Alkoin	24/02/1981	Greece	Xilikastro	N-S	6.7	IX	0.290	3.59	0.57
GM4	Friuli	06/05/1976	Italy	Tolmezzo	E-W	6.3	IX	0.315	6.32	1.00
GM5	Tabas	16/09/1978	Iran	Boshroych	N79E	7.3		1.004	1.91	0.30
GM6	Campano Lucano	23/11/1980	Italy	Irpinia,Calitri	E-W	6.7	VIII	0.175	2.83	0.45
GM7	Lazio - Abruzzo	07/05/1984	Italy	Cassino-Sant'Elia	N-S	5.8	VII	0.110	1.69	0.26
GM8	Kocaeli	17/08/1999	Turkey	Yesilkoy	N-S	7.8		0.089	2.16	0.34
GM9	Gazli	17/05/1976	Uzbekistan	Gazli	E-W	7.0		0.720	9.18	1.45
GM10	Montenegro	15/04/1979	Montenegro	Bar-S.O.	E-W	7.0		0.363	6.92	1.10

3.2 Joint and beam characterization

The correct modelling of the semi-rigid, partial strength composite joint, along with the modelling of the composite beams, is of maximum relevance when evaluating the seismic performance of the frame. Most of the plastic dissipation energy, in fact, takes place in these elements.

√ The main sources of uncertainty for the frame are listed in the following:

√ geometry of structural parts;

√ intensity and type of loads;

√ mechanical properties of materials;

√ type of hysteresis loop of the structural joints and plastic hinges in the beams.

In this paper, the attention has been focused on the mechanical properties of materials and on their influence on the strength of the joints and composite beams. Permanent and variable loads, as well as the geometry of the structure, will be regarded as deterministic, their degree of uncertainty being negligible compared to that of the seismic action. Instead the yield stresses of construction steel and rebars, as well as the ultimate stresses of concrete, bolts and stud connectors have been assumed as random variables, which are characterized by a statistical distribution.

1) Construction steel

Mechanical properties of steel profiles are affected by both random phenomena and production processes. According to Piluso *et al* (2003), the statistical distribution of the yield stress f_y has been assumed as dependent on the thickness of the plates which make up the profile. It was pointed out that the Lognormal distribution best represents the experimental distribution. Furthermore, the mean of the logarithm of the yield stress can be considered as linearly dependent on the thickness t , with decreasing trend:

$$E(\ln f_y) = c_1 - c_2 t = 5.766 - 0.007t \quad (4)$$

where c_1 and c_2 are material parameters dependent on the type of steel, t is the thickness in mm, and f_y is the yield stress in N/mm^2 . Table 2 summarizes the statistical parameters of the random variables employed for the beams and columns of the frame tested at Ispra, where:

- $f_{y,m}$ is the mean value of the yield stress;
- s is the standard deviation of the yield stress;
- λ and ξ are, respectively, the mean value and the standard deviation for the lognormal distribution:

$$\lambda = \ln f_{y,m} - \frac{\xi^2}{2}, \quad \xi = \sqrt{\ln(COV^2 + 1)} \quad (5)$$

Table 2 Statistical parameters for the joint components

Steel components (Fe 360)	t [mm]	λ	ξ	COV	$f_{y,m}$ [N/mm ²]	s [N/mm ²]
column flange	HEB260	17.50	5.64	0.07	283.1	19.8
column web	HEB260	10.00	5.70	0.07	298.4	20.9
column flange	HEB280	18.00	5.64	0.07	282.2	19.8
column web	HEB 280	10.50	5.69	0.07	297.4	20.8
beam flange	IPE 300	10.70	5.69	0.07	296.9	20.8
beam web		7.10	5.72	0.07	304.5	21.3
End plate		15.00	5.66	0.07	288.1	20.2

– COV is the coefficient of variation defined as:

$$COV = \frac{s}{f_{y,m}} \quad (6)$$

2) Rebars

The coefficient of variation generally reported in literature for rebars lies in the range 4% to 12%. Either normal or lognormal statistical distributions are employed by different authors. In this paper, a lognormal distribution with a COV equal to 6% has been assumed, according to Altug and Elnashai (2004). In the Table 3 the statistical properties are summarised.

3) Concrete

It is generally accepted in literature that the compression strength of concrete (f_c) may be represented by a normal distribution. Dymitiotis *et al.* (1999) suggest a coefficient of variation of 15% for such a quantity. The mean value can be obtained from the characteristic strength of the material using the equation:

$$f_{c,m} = \frac{f_{c,k}}{1 - k \cdot COV}, \quad k = 1.64 \quad (7)$$

In the Table 3 the statistical properties used for concrete are reported.

4) Bolts

The ultimate strength of bolts in tension has been considered as normal distributed with mean value $E(f_u) = 1.2 \cdot f_{u,k}$, and coefficient of variation of 2% (Piluso *et al.* 2003). In the Table 3 the adopted statistical properties are shown.

5) Stud connectors between steel beam and r.c. slab

A normal distribution with coefficient of variation of 4% has been considered. The mean value of the ultimate strength has been obtained from the corresponding characteristic value. In the Table 3 their statistical properties are reported.

Based on the aforementioned mechanical properties of the materials, the strengths of joints and beams, regarded as stochastic variables, have been computed through a Monte Carlo simulation. Two different cases have been considered:

- Plasticization of the beam-to-column composite joints, i.e., evaluation of the plastic resistant moments, under positive and negative bending, for the exterior and interior joints;
- Plasticization of the composite beams, i.e., evaluation of the plastic resistant moments, under sagging and hogging bending, for the 5 m and 7 m bay beams.

Table 3 Statistical parameters for used materials

Material	COV	f_m [N/mm ²]	s [N/mm ²]
Rebars Fe b 44k (B450 C)	0.06	477.09 ($f_{y,m}$)	28.63
Concrete Class C25/30	0.15	38.43 ($f_{c,m}$)	5.76
Bolt Class 10.9	0.02	1070.0 ($f_{u,m}$)	21.4
Stud Nelson 3/4"	0.04	553.4 ($f_{u,m}$)	22.1

3.2.1 Statistical simulation

The Monte Carlo simulation has been used to calculate the plastic resistant moment of the composite beam according to the Eurocode 4 (1992). A number of 10000 pseudo-random values in accordance with the statistical distributions previously defined has been generated for each random variable using the Box and Muller method (Augusti *et al.* 1984). The mean values $M_{pl,m}$, standard deviations s , and coefficients of variation COV of the plastic resistant moments have then be computed. Through some statistical tests, like the χ^2 and the K-S, Kolmogorov-Smirnov tests, (see Benjamin and Cornell 1970, Rubinstein 1981), it has been pointed out that the best probability distribution function fitting with the obtained statistics is the lognormal one. Obtained results are reported in Table 4 for the 5 m bay composite beam. Analogous results have been obtained for 7 m bay composite beam.

The beam-to-column exterior and interior joints have been schematised using the component models depicted in Figs. (3a) and (3b), respectively.

In this model all the axial springs are characterised by three-linear relationships with no degradation of stiffness and strength under cyclic loading. The relevant points of the relationships for the steel and concrete slab components have been evaluated according to the Annex J of Eurocode 3 (1994) and Eurocode 4 (1996), and according to Faella *et al.* (1998, 2000). The composite joints have then been analysed using the Abaqus Finite Element code (Hibbit *et al.* 1997). The experimental-numerical comparison, in terms of moment M and rotation θ , is reported in Figs. 4(a) and 4(b) for the exterior and interior joints, respectively, which were tested under monotonic loading at the Universities of Pisa and Milan (Salvatore *et al.* 2004). An overall good correspondence can be noted in both diagrams.

Table 4 Statistical parameters of the composite beam under bending moment

Bending Moment	$M_{pl,m}$ [KN/m]	s [KN/m]	λ	ξ	COV
Sagging	426,62	20,38	6,055	0,048	0,05
Hogging	252,79	10,94	5,532	0,043	0,04

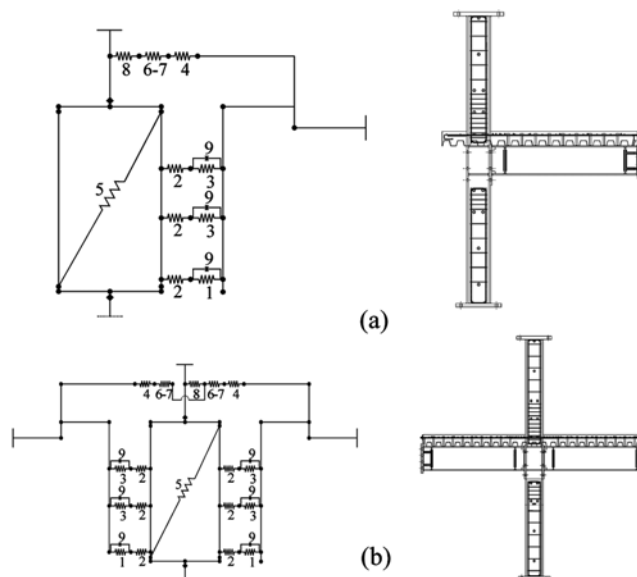


Fig. 3 Component model for exterior (a) and interior (b) joint

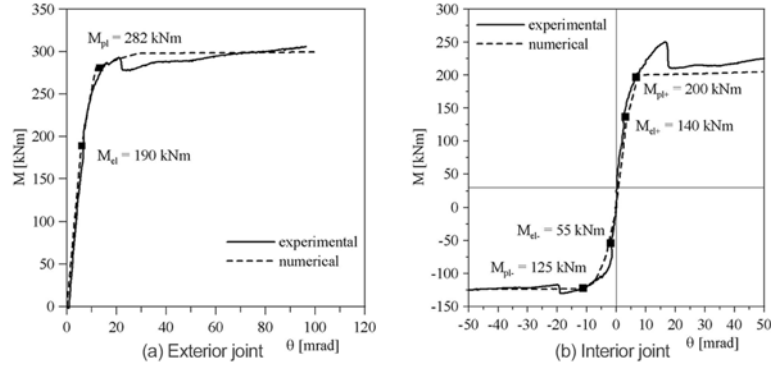


Fig. 4 Experimental-numerical comparison for (a) exterior joint, and (b) interior joint

Since the computational time required for the statistical simulation of a composite joint is much higher than for a composite beam, an optimised Monte Carlo simulation has been used. The stratified sampling technique, also known as the Latin Hypercube Sampling (Olsson *et al.* 2003), has been employed. The advantage of this technique is the possibility of reducing the number of analyses without notable reduction of accuracy. The random variables considered in this study are: (1) yield stress of the HEB column flanges, f_{ycf} ; (2) yield stress of the HEB column web, f_{ycw} ; (3) yield stress of the IPE beam flanges, f_{ybf} ; (4) yield stress of the IPE beam web, f_{ybw} ; (5) yield stress of the endplate, f_{yep} ; (6) yield stress of the rebars, f_{sr} ; (7) cylindrical compression strength of concrete, f_c ; (8) ultimate strength of Nelson studs, f_{us} ; (9) ultimate strength of bolts, f_{ub} . The adopted procedure is summarised in the following:

- 1) the interval of cumulative probability [0,1] has been divided into 200 sub-intervals of equal probability;
- 2) a random number in the range [0,1] has been generated for each random variable and each sub-interval. 200 values of probability density have been obtained for each variable;
- 3) the values of the random variables have then been obtained from the 200 values of probability density once their statistical distribution have been assumed;
- 4) each of the 200 values of the random variables above calculated has been randomly coupled with the other 8 different variables. In this way 200 vectors of 9 parameters each, which fully characterise the mechanical properties of the joints, have been achieved;
- 5) the strength of each component (spring) of the joint model has been computed as described above, assuming the stiffness as a deterministic variable. Such values have then been employed in the Abaqus schematisation of the joint in order to determine the statistical distribution of the resisting moment. A number of 200 exterior and 200 interior joints subjected to positive and negative moments have been analysed.

The statistical tests of χ^2 and of Kolmogorov-Smirnov have proved that the lognormal probability distribution function *PDF* better represents the joint strength statistics. Fig. 5 depicts, as an example, the frequency histograms for the strength of the internal joint subjected to positive moment and external joint subjected to negative moment. Fig. 6 shows the convergence of the approach in terms of ratios between the current mean value and standard deviation with the correspondent final values, incrementing the number N of samples. By only 200 samples the convergence is reached, whereas, in general, with the Monte Carlo approach a very high number of samples are necessary (5000÷7000). The statistical values of the resistant moment in terms of mean value M_r , standard deviation s and coefficient of variation *COV* are displayed in Table 5.

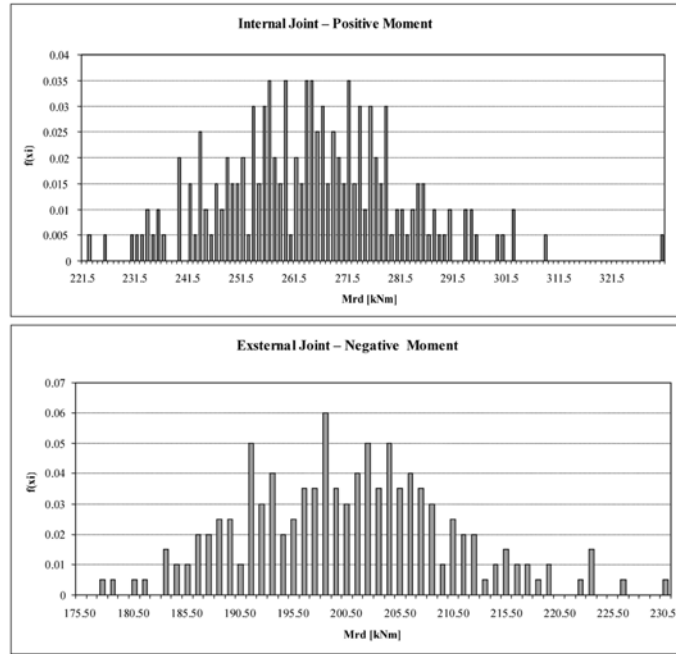


Fig. 5 Frequency histograms of joints

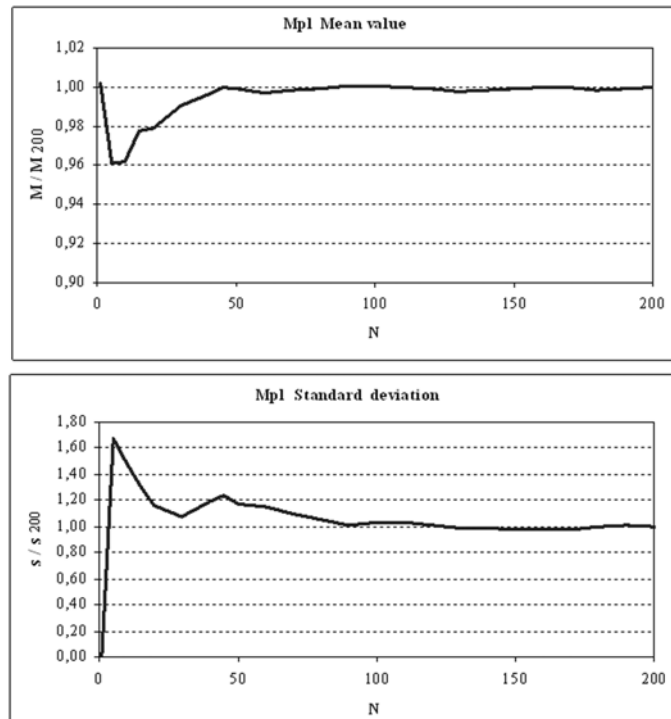


Fig. 6 Convergence of the Latin approach for the internal joint-positive moment

Table 5 Statistical parameters for the composite joints

Type of joint	Bending	Macro-model		
		M_r [kNm]	s [kNm]	COV
External	$M > 0$	263.86	16.87	0.06
	$M < 0$	200.14	9.74	0.05
Internal	$M > 0$	178.07	10.09	0.06
	$M < 0$	107.34	8.61	0.08

The results of the statistical analyses described above have been used to analyse the entire composite frame. In order to reduce the computational time needed in a non-linear time-history analysis of the frame, the composite joints have been modelled using the rotational spring (link element) provided by SAP2000 version 9.1 code, and characterised by a bilinear global moment-rotation relationship. The resistant moments (positive and negative) have been assumed as random variables and computed on the basis of the results described above, while the stiffness has been considered as a deterministic quantity.

3.3 Frame analysis

In order to draw the fragility curves of the frame, the damage parameters must be identified, along with the values assumed by such quantities when the different performance levels are achieved. The interstorey drift angle $ISDA$, which is given for a frame by:

$$ISDA = \max_{i=1}^n \left(\frac{\delta_i}{h_i} \right) \quad (8)$$

where n is the number of stories, δ_i is the interstorey drift, and h_i the interstorey height, has been considered in the paper. This parameter is the most used since it is well correlated with the damage of structural and non structural elements, and in general it is adopted by codes to control the damage in simple way.

Table 6 reports the limit values employed for the $ISDA$ damage parameter corresponding to the achievement of a given degree of damage in the frame. These values have been calibrated on the maximum rotation of plastic hinges and joints according to Eurocode 8 (2004), that for performance levels LS1, LS2, LS3, are equal to 13, 30, 50 mrad, respectively. Such limit points are reported in Fig. 7, where a good correspondence with the assumed limit rotations is pointed out. The pushover curve has been drawn for the frame tested at ISPRA by assuming a distribution of lateral forces proportional to the storey masses. The frame has been schematised according to the FE model depicted in Fig. 8. The analysis has been carried out by using the non-linear FE software SAP2000, assuming the actual mechanical properties of the frame tested at ISPRA.

In the probabilistic analysis the strength of the joint has been considered as a random variable and

Table 6 Damageability limit states expressed through the $ISDA$ index

Level of damage	$ISDA$ %	Consequence
LS0 : REDUCED	0.5	Usable building
LS1 : LIMITED	1.0	Repairable building
LS2 : SIGNIFICANT	2.5	Irrecoverable building
LS3 : NEAR COLLAPSE	5.0	Loss of the building

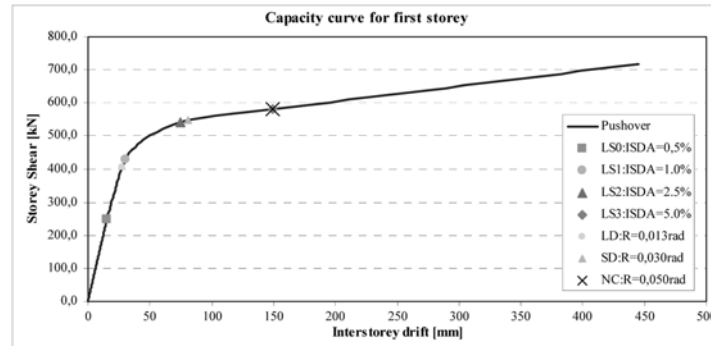


Fig. 7 Comparison among the damageability limit states defined through the *ISDA* index and limit rotation of EC8

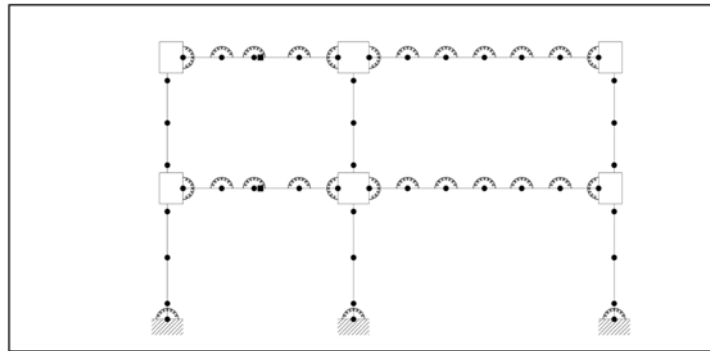


Fig. 8 FE model adopted for the frame

computed using the statistical simulation described in the previous paragraph on the basis of the statistical distribution of the material mechanical properties. In particular, the beam-to-column joint has been modelled using a link element with bilinear non-symmetric moment-rotation relationship. The elastic stiffness for positive and negative bending was obtained through the component method and considered as a deterministic variable. In plastic phase, the joint has been considered perfectly plastic, with stable loops without pinching.

The composite beams have been modelled by means of elastic beam elements linked one to another with rigid-plastic rotational springs without pinching. The strength of such springs has been considered as a random variable and computed using the statistical simulation. The columns have been modelled with linear beam elements and connected to the foundation with an elasto-plastic rotational spring.

The FE model of the frame has been validated against the results of the pseudo-dynamic tests performed at ISPRA (Bursi *et al.* 2004). Fig. 9 displays the experimental-numerical comparison for a generated earthquake ground motion compatible with the Eurocode 8 spectrum in the case of type A soil and 0.25 g *PGA*. The numerical results have been carried out using the fast-nonlinear time-history analysis with a structural damping ratio $\xi = 5\%$. Despite the simplicity of the model adopted for the joint in dynamic conditions, an overall fairly good accuracy can be noted, however the numerical model underestimates the damping of the structure towards the end of the analysis.

Once validated the FE model, a sample of 15 pseudo-random frames has been generated using the stratified Latin Hypercube Sampling method with 9 random variables: strength of the column-to-foundation

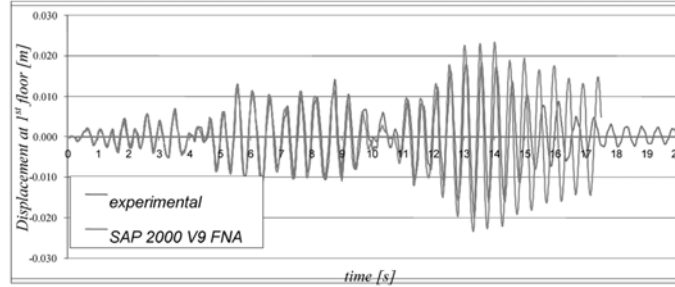


Fig. 9 Experimental-numerical comparison for $PGA = 0.25g$

joint, characterised by a log-normal distribution with mean value $\lambda = 5.64$, standard deviation $\zeta = 0.07$ and coefficient of variation $COV = 0.07$; positive and negative ultimate moments for the 5 m and 7 m bay beams, characterised by a log-normal distribution with mean value, standard deviation and coefficient of variation reported in Table 4; positive and negative ultimate moments for the interior and exterior beam-to-column joints, characterised by a log-normal distribution with mean value, standard deviation and coefficient of variation reported in Table 5. The earthquake, as discussed in the introduction, is the main source of uncertainty, since the corresponding recorded ground motion is uncertain in terms of peak ground acceleration PGA , duration, and frequency content. Such uncertainties have been taken into account by subjecting the 15 frames generated above to the 10 recorded ground motions selected in paragraph 3.1 and summarised in Table 1. The corresponding displacement response spectra computed for a damping ratio $\xi = 5\%$ are displayed in Fig. 10. Each ground motion, described by the history of ground acceleration, has been scaled on 10 values of seismic intensity, represented by the spectral displacement S_{di} . Such a quantity is commonly regarded as the most stable and representative parameter of the seismic intensity (Bazzurro and Cornell 1994, Altug and Elnashai 2004). The scale factors have been selected so that the frames can achieve all the damage levels previously defined. The displacement response spectrum of each earthquake has been scaled with the factor λ_i , $i = 1$ to 10, such that the spectral displacements S_{di} corresponding to the natural vibration period of the frame ($T_1 = 0.506s$) are equal to 20, 30, 40, 50, 60, 80, 100, 120, 160, and 200 mm. The adopted procedure can be summarised in the following:

- (1) the interval of cumulative probability $[0,1]$ has been divided into 15 sub-intervals of equal probability;
- (2) a random number in the range $[0,1]$ has been generated for each random variable and each sub-interval. 15 values of probability density have then been obtained for each variable;

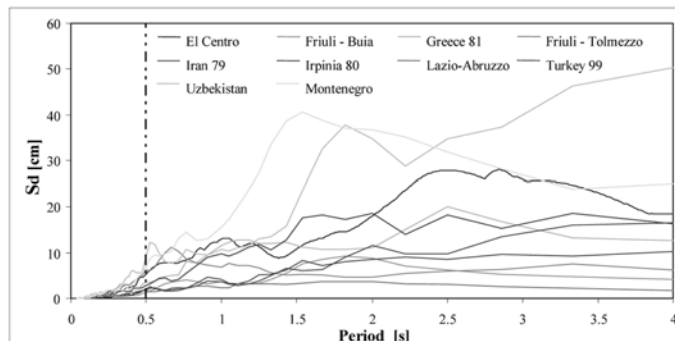


Fig. 10 Displacement spectra ($\xi = 5\%$) for the selected earthquake ground motions.

- (3) the values of the random variables have then been achieved from the 15 values of probability density once their statistical distribution have been assumed;
- (4) each of the 15 values of the random variables above calculated has been randomly coupled with the other 8 different variables. In this way 15 vectors of 9 parameters each, which fully characterise the mechanical properties of the frames, have been obtained;
- (5) All of the 15 frames have then been subjected to the 10 earthquake ground motions, each of them scaled through the factor λ_i to the 10 values of seismic intensity corresponding to S_{di} . An overall number of 1500 ($15 \times 10 \times 10$) nonlinear time-history analyses have then been carried out.

Fig. 11 displays, as an example, the structural response of the frame in terms of Incremental Dynamic Analysis (see Mwafy and Elnashai 2001, Vamvatsikos and Cornell 2002), for the earthquake recorded at Tolmezzo, Friuli (Italy), in 1976. The (*IDA*) curve, which reports the maximum base shear versus the maximum top floor displacement for different values of *PGA*, is also known as the dynamic pushover curve. Such a curve is also compared with the outcomes of static pushover analyses (*SPA*) carried out in the cases of lateral forces proportional to the masses (uniform distribution) and proportional to the first vibration mode (inverted triangular distribution). Fig. 12 reports the comparison in terms of *IDA* among different earthquake ground motions. The main remarks are reported herein after:

- (1) the *IDA* curves markedly depends on the type of earthquake ground motion;
- (2) for *PGA* less than 0.5 g, the *IDA* curves generally fit with the *SPA* curves with lateral forces proportional to the masses. This is true for almost all ground motions;
- (3) for *PGA* larger than 0.5 g to 0.8 g, the *IDA* curves lie well above the *SPA* curves, especially for the Uzbekistan, Lazio-Abruzzo, Turkey and Montenegro ground motions;
- (4) the limit state of reduced damage LS0 is achieved, on average, for *PGA* in the range from 0.1 g to 0.15 g;
- (5) the limit state of limited damage LS1 is achieved, on average, for *PGA* in the range from 0.25 g to 0.35 g;
- (6) the limit state of significant damage LS2 is achieved, on average, for *PGA* in the range from 0.70 g to 1.00 g; the limit state of near collapse LS3 is achieved, on average, for *PGA* larger than 1.30 g.

The fragility curves have been obtained as a result of the 1500 nonlinear time-history analyses above described, the outcomes of which have been analysed using the statistical approach. Fig. 13 displays the

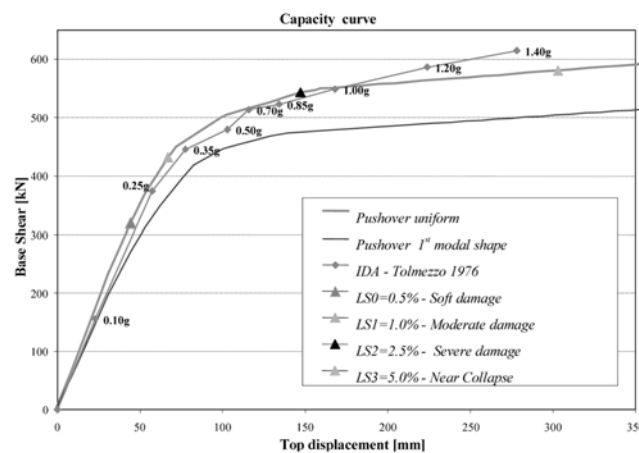


Fig. 11 Comparison among static pushover and dynamic pushover of the Tolmzzo (1976) ground motion

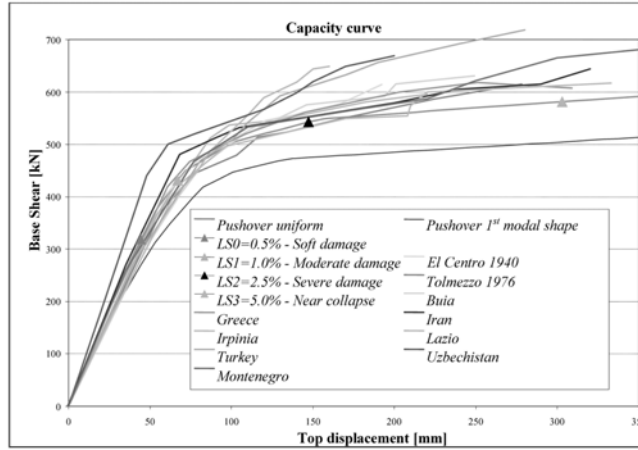


Fig. 12 Comparison among the dynamic pushover curves for different earthquake ground motions

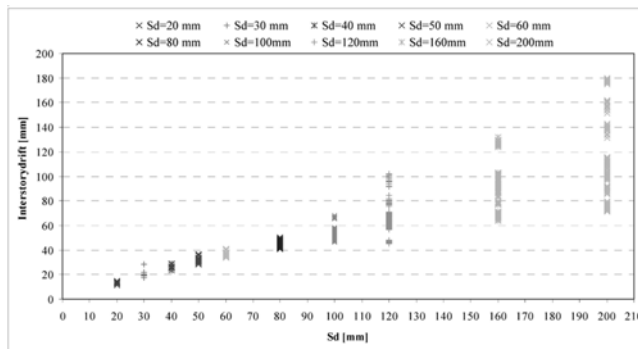


Fig. 13 Outcomes of the time-history analyses in terms of interstorey drift versus spectral displacement.

outcomes carried out for the frame using the interstorey drift as damage parameter.

150 values of the *ISDA*, carried out by subjecting each of the 15 frames to 10 ground motions, are reported for each of the 10 adopted spectral displacements, which represent the seismic intensity. This damage parameter has then been regarded as a random variable at each level of seismic intensity. According to the literature (Dymitiotis *et al.* 1999, Piluso *et al.* 2003, Altug and Elnashai 2004), a lognormal distribution has been assumed to represent the damage parameter at each level of spectral displacement S_d . Figs. 14 and 15 display the probability density functions obtained for the limit states defined on the basis of the global damage index *ISDA* for the values $S_d = 50$ mm and $S_d = 200$ mm, respectively.

The accuracy of the adopted lognormal distributions has been checked using the Kolmogorov-Smirnov test. It has been found that the lognormal distributions satisfy the accuracy level up to the seismic level $S_d = 80$ mm, while for higher levels the test is no longer satisfied. This result can be justified because of the large scatter of values for higher seismic intensities, mainly due to the increased influence of the uncertainties affecting the mechanical properties of materials when the structure largely deforms in plastic phase.

Through a fitting by using a log-normal distribution, the fragility curves with *ISDA* as damage parameter, have been obtained. Such curves, displayed in Fig. 16, represent the cumulative probability

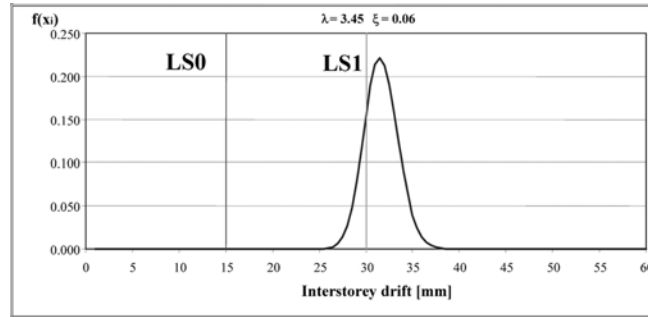


Fig. 14 Lognormal probability distribution function of the *ISDA* damage parameter obtained for the 4th level of seismic intensity $S_d = 50$ mm

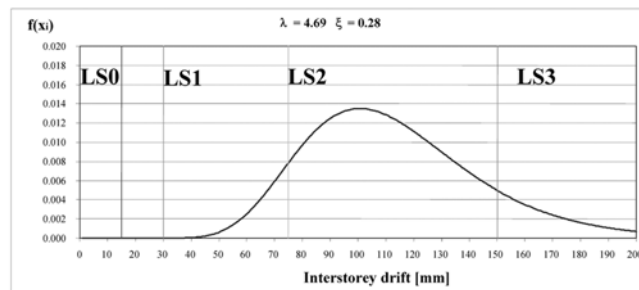


Fig. 15 Lognormal probability distribution function of the *ISDA* damage parameter obtained for the 10th level of seismic intensity $S_d = 200$ mm

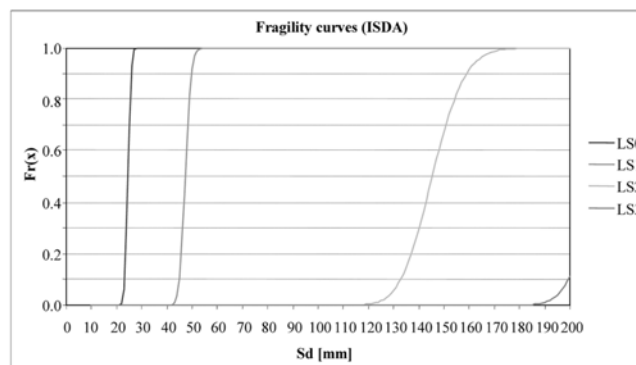


Fig. 16 Fragility curves (*ISDA*) in terms of S_d for different damage limit states

distributions of a given damage limit state when the seismic intensity, represented by the spectral displacement, is assumed as a random variable.

The same fragility curves are reported in Fig. 17 in terms of *PGA* (obtained as medium *PGA* of the scaled earthquakes for a fixed S_d value).

The trends of the fragility curves in terms of *ISDA* demonstrate that the frame is subjected to significant interstorey drifts even for low seismic intensities. Table 7 reports the probability F_r of

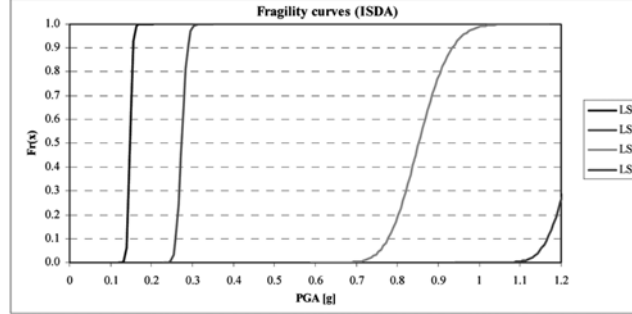


Fig. 17 Fragility curves (*ISDA*) in terms of *PGA* for different damage limit states

reaching a given damage limit state once a seismic event with a pre-fixed intensity occurs. The seismic intensity has been represented by the spectral displacement S_d . Some values corresponding to medium *PGA* for the set of ground motions used in the analyses have been selected for S_d and reported in Table 7. The values of probability F_r have been obtained from curves of Figs. 16, 17.

It is worth highlighting that the values of probability F_r do not represent the actual probability of failure for the structure since such probability will depend also on the seismic hazard of the region where the structure is located. In order to calculate the failure probability, the curve of seismic hazard must be introduced. Such a curve provides the annual probability of exceeding of a given seismic intensity (see Eq. 3), which is generally measured by the spectral acceleration S_a . In order to calculate the probability of failure for the frame under study, the seismic hazard curve proposed by Song and Ellingwood (1999) for the state of California has been considered. Such a curve, represented by Eq. (3) with parameters $k = 2.38$ and $\mu = 0.045$, provides values of seismic hazard compatible with those of the Irpinia earthquake-prone region (Italy). The failure probabilities P_f are reported in Table 8 in terms of *ISDA*. In such table, the quantities λ and ξ correspond to the parameters of the lognormal distributions representing the fragility curves, while the quantities μ_{S_d} and μ_{S_a} denote the mean values of S_d and S_a . The correspondent performance curve is displayed in Fig. 18. Such curve defines the annual probability of exceeding with reference to the damage that the structure may suffer in a fixed earthquake-prone region. Hence, the performance curves can be considered as the final outcome of a reliability analysis carried out using a full probabilistic approach.

Table 7 Probability F_r of reach of a given damage limit state for the frame tested at *ISPRA*

		LS0	LS1	LS2	LS3
<i>ISDA</i>	S_d	23 mm	42 mm	113 mm	175 mm
	<i>PGA</i>	~0.1 g	~0.25 g	~0.6 g	~1.0 g
	F_r	6.02E-02	1.44E-03	1.61E-04	1.35E-05

Table 8 Probabilities of failure for the frame based on the use of the *ISDA* parameter

	<i>ISDA</i> [%]	ξ	λ	μ_{S_d} [mm]	μ_{S_a} [g]	P_f
LS0	0.5	0.041	3.198	24.52	0.4	6.1×10^{-3}
LS1	1.0	0.040	3.856	47.33	0.7	1.3×10^{-3}
LS2	2.5	0.070	4.979	145.71	2.3	8.8×10^{-5}
LS3	5.0	0.045	5.353	211.39	3.3	3.6×10^{-5}

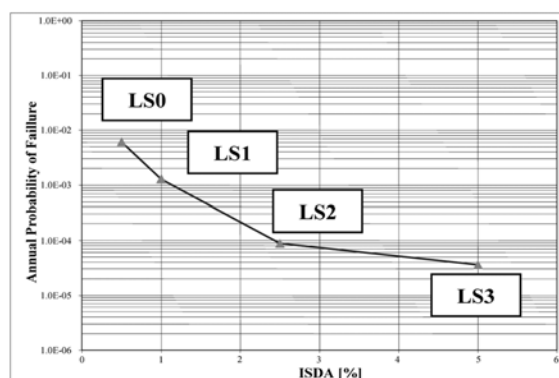


Fig. 18 Performance curve of the structure based on the use of the *ISDA* parameter

4. Conclusions

In the paper, the seismic performance of a partially-restrained steel-concrete composite frame, has been investigated by means of a full probabilistic approach. The frame was designed using the Eurocode 8 and tested at the ELSA laboratory of the Joint Research Centre of Ispra (Italy).

Statistical tests have proved that the lognormal probability distribution function, better represents the obtained statistics of the joints and beams strength. For the analysed joints and beams, the *COV* lies in the range 5%÷8% and 4÷5%, respectively.

For the whole frame, the fragility and performance curves have been obtained using the Latin Hypercube Sampling tool, carrying out 1500 nonlinear time-history analyses. In order to evaluate the performance of the analysed composite frame, on the basis of the probabilistic analysis, an acceptable value of the annual probability of exceeding must be defined for each of the four damage limit states. Accepting the following usual values: LS0 → 10^{-2} ; LS1 → 10^{-3} ; LS2 → 10^{-4} ; LS3 → 10^{-5} , from Table 8 it can be noted that the frame exhibits an annual probability of exceeding of $6.1 \cdot 10^{-3}$, $1.3 \cdot 10^{-3}$, $8.8 \cdot 10^{-4}$, and $3.6 \cdot 10^{-5}$ for the reduced (LS0), limited (LS1), significant (LS2), and near collapse (LS3) damage limit state, respectively. It can be then observed that the frame is slightly under-designed for the LS2 and LS3, while it is slightly over-designed for the reduced and limited damage limit states. This result is in contrast with the design of the frame obtained using the static analysis according to the Eurocode 8 deterministic approach. In this case, in fact the serviceability limit states were the most critical conditions.

Another important point revealed by the probabilistic analysis is that the acceptable values for the *PGA* at the collapse are around 1.0 g (see Table 7 and Fig. 17). Conversely, the deterministic analysis based on the static or dynamic pushover (see Fig. 11 for example), can overestimate the resistance of the frame, leading to *PGA* larger than 1.4 g. This is owed to the large scattering of dynamic results when the seismic intensity increases. The design value of Eurocode 8, for a return period of 475 years (0.40 g), has been in any case assured.

References

- Altug Erberik, M. and Elnashai Amr, S. (2004), "Fragility analysis of flat-slab structures", *Eng. Struct.*, Elsevier, 937-947.

- Augusti, G., Baratta, A. and Casciati, F. (1984), *Probabilistic Methods in Structural Engineering*, Chapman & Hall, London.
- Bazzurro, P. and Cornell, C. A. (1994), "Seismic hazard analysis of square confined concrete columns", *J. Struct. Div*, ASCE 1982; ST 4; 929-50.
- Benjamin, J. and Cornell, C. A. (1970), *Probabilistic, Statistics and Decision for Civil Engineers*, McGraw-Hill, New-York.
- Bertero, R. D. and Bertero, V. V. (2002), "Performance-based seismic engineering: the need for a reliable conceptual comprehensive approach", *Earthq. Eng. Struct. Dyn.*, **31**(3), 627-652.
- Bursi, O. S., Caramelli, S., Fabbrocino, G., Molina, J., Salvatore, W., Taucer, F., Tremblay, R. and Zandonini, R., (2004), "3D Full Scale Seismic Testing of a Steel-Concrete Composite Building at ELSA", Report, Institute for the Protection and the Security of the Citizen, European Laboratory for Structural Assessment (ELSA), Ispra (VA).
- CEN, European Committee for Standardisation (1992), "Eurocode 4. Common Unified Rules for Composite Steel and Concrete Structures", ENV 1994-1-1, Brussels.
- CEN, European Committee for Standardisation (1994), "Eurocode 3. Proposed Annex J for ENV 1993-1-1", Brussels.
- CEN, European Committee for Standardization (1994), "Eurocode 8. Design provisions for earthquake resistance of structures", Brussels.
- CEN, European Committee for Standardisation (1996), "Eurocode 4. Proposed Annex J for ENV 1994-1-1", Brussels.
- CEN, European Committee for Standardisation (1996), "Eurocode 8. Design provisions for earthquake resistance structure", ENV 1998-1-1, Brussels.
- Cornell, C. A. and Krawinkler, H. (2000), "Progress and challenges in seismic performance assessment", <http://peer.berkeley.edu/news/2000spring/performance/html.febwetg4wt4>.
- Dymitiotis, C., Kappos, A. J. and Chryssanthopoulos, M. K. (1999), "Seismic reliability of RC frames with uncertain drift and member capacity", *J. Struct. Eng.*, ASCE, **125**(9), 1038-47.
- Faella, C., Piluso, V. and Rizzano, G. (1998), "Experimental analysis of bolted connections: Snug versus preloaded bolts", *J. Struct. Eng.*, ASCE, **124**(7), 765-774.
- Faella, C., Piluso, V. and Rizzano, G. (2000), *Structural Steel Semirigid Connections*, CRC PRESS.
- FEMA 273. (1997), "NEHRP Guidelines for the seismic rehabilitation of buildings", Federal Emergency Management Agency, Washington.
- FEMA 356. (2000), "Prestandard and commentary for the seismic rehabilitation of buildings", Federal Emergency Management Agency, Washington.
- Hibbit, Karlsson & Sorensen Inc. (1997), Abaqus, Version 5.7, U.S.A.
- Mwafy, A. M. and Elnashai A. S. (2001), "Static pushover versus dynamic collapse analysis of RC buildings", *Eng. Struct.*, **23**, 407-424.
- Olsson, A., Sandberg, G. and Dahlblom O. (2003), "On Latin hypercube sampling for structural reliability analysis", *Structural Safety*, Elsevier, **25**, 47-68.
- Park, Y. J., Ang, AH-S. and Wenn, Y. K. (1985), "Mechanistic seismic damage model for reinforced concrete", *J. Struct. Eng.*, ASCE, **111**(4), 722-739.
- Piluso V., Rizzano G. and Totoli G. (2003), "Progettazione a completo ripristino di resistenza di collegamenti flangiati trave colonna: approccio probabilistico", *Costruzioni Metalliche*, LV(2003), n. 1.
- Rubinstein R. Y. (1981), *Simulation and the Monte Carlo method*, John Wiley & Sons.
- Sakurai S., Ellingwood B. and Kushiyaama S. (2001), "Probabilistic study of the behaviour of steel frames with partially restrained connections", *Eng. Struct.*, **23**(2001), 1410-1417.
- Salvatore, W., Braconi, A., Bursi, O. S. and Trambly, R. (2004), "Partial Strength beam-to-Column Joint for High Ductile Steel-Concrete Composite MR Frames", Paper n° 2829 of the 13th World Conference on Earthquake Engineering, Vancouver, B.C., Canada, August.
- Sap2000 version 9.1 (2004), Computer and Structures, Inc, Berkeley, CA.
- SEAOC, Structural Engineers Association of California (1995), "Vision 2000, Performance-based seismic engineering", Sacramento, CA.
- Song, J. and Ellingwood, B. R. (1999), "Seismic reliability of special moment steel frames with welded connections", *J. Struct. Eng.*, ASCE, **125**(4), 372-384.
- Vamvatsikos, D. and Cornell, C. A. (2002), "Incremental dynamic analysis", *Earthq. Eng. Struct. Dyn.* **3**, 491-514.